Progress In Electromagnetics Research M, Vol. 71, 127–136, 2018

Dual-Band UHF RFID Tag Antenna Using Two Eccentric Circular Rings

Bidisha Barman, Sudhir Bhaskar*, and Amit Kumar Singh

Abstract—A low profile dual-band passive Ultra High Frequency Radio Frequency Identification (UHF RFID) tag antenna designed to operate at two RFID bands allocated for use in Europe (865–868 MHz) and Japan (950–956 MHz) is proposed. The antenna has two eccentric circular rings of different radii to provide dual band response. An arc-shaped strip with Impinj Monza-4 IC chip is used to feed the two rings simultaneously by microstrip-line coupling-feed technique. The proposed design is simulated using Ansoft HFSS, and the prototype is fabricated. The return losses at 866 MHz and 952 MHz are measured to be −12.25 dB and −12.99 dB, respectively, which are in good agreement with the simulated results. The proposed antenna exhibits a 10 dB bandwidth of 9 MHz from 862 to 870 MHz and an 8 MHz 10 dB bandwidth from 949 to 956 MHz covering the UHF RFID bands in Europe and Japan. The maximum read ranges are measured to be around 3 m in the 865–868 MHz band and 2.6 m in the 950–956 MHz band.

1. INTRODUCTION

Of late, Radio Frequency Identification (RFID) system has turned out to be one of the most popular automatic identification techniques, replacing the omnipresent barcodes in an increasing number of cases. It has found widespread application in supply chain management, health care, inventory, animaltracking, and security [1]. An RFID system consists of an electronic data-carrying device called the tag, an interrogator or reader, and a host computer with application software. Tags can be active (with on board source of power, like battery) or passive (without battery). A typical passive tag comprises an antenna and an IC chip. For practical applications, RFID tag antennas must be small, low profile, and suitable for low-cost mass production.

Generally four frequency bands are used for RFID systems; i.e., low frequency (125–134 kHz), high frequency (13.56 MHz), ultra-high frequency (860–960 MHz) and microwave frequency (2.45, 5.8 and 24 GHz) [2]. The ultra high frequency (UHF) tags have garnered more attention as they offer longer read ranges, higher reading speeds, enable simultaneous detection of more number of tags and need smaller antennas than low frequency (LF) and high frequency (HF) systems [3]. Transfer of data between the tag and the reader is achieved by near-field coupling with load modulation in LF and HF bands, whereas, in UHF bands, the principle of backscatter modulation is used [4]. In backscatter modulation, the tag antenna receives the modulated signal transmitted by the reader. The RF voltage developed across the antenna terminals powers up the chip. The chip acts as a switch to match or mismatch its internal load to the antenna by varying its input impedance leading to the effective modulation of the backscattered signal [5].

Different parts of the radio spectrum have been allocated by different countries for RFID, viz. 866–869 MHz in Europe, 902–928 MHz in North and South America, and 950–956 MHz in Japan [6]. One of the important challenges is to design tags which can be operated at any two or more of these

Received 20 June 2018, Accepted 26 July 2018, Scheduled 1 August 2018
* Corresponding author: Sudhir Bhaskar (sbhaskar.rs.ece@iitbhu.ac.in).
The authors are with the Department of Electronics Engineering, Indian Institute of Technology (BHU), Varanasi, India.

regulated UHF bands simultaneously. The tags which are capable of operating at two of the allocated frequencies simultaneously are referred to as dual-band tags. The dual-band tags are proposed as an alternative to broadband tags, as they provide better matching at two specific bands and higher read ranges than the later [7]. Several methods to obtain dual-band behaviour have been reported earlier in literature. One of the techniques is the simultaneous excitation of two orthogonal modes, i.e., TM_{01} and TM_{10} at the first and second resonant frequencies respectively [8] by proper selection of the feed location. The use of multiple patches to generate dual bands is reported in [9, 10]. In these structures, each of the multiple patches of different resonant lengths supports strong currents and radiations at different resonant frequencies, hence providing dual-band behaviour. Dual-band response can also be obtained by introducing reactive loads, such as stubs [11], notches [12], and slots [13] to a single patch, wherein the current distribution of one of the modes of the patch is modified to alter the resonant frequency of that particular mode without significantly affecting the other mode. Perturbation method to obtain dual-band response has been reported by Paredes et al. in [14]. In this method, spiral or split ring resonators coupled to a mono-band antenna (resonating at an intermediate frequency f_0) split the tag resonance into two (one beyond and the other below f_0) by perturbing the line impedance and electrical length of the antenna. Some of other methods to achieve dual-band response involve the use of AMC ground plane [15] in which the reflection phase of the ground plane is changed to obtain double resonance at two required frequencies of the material.

In this paper, a new low profile UHF RFID dual-band tag antenna consisting of two eccentric circular rings with a short-circuited arc-shaped feeding strip in between is presented. The outer ring resonates at 866 MHz, and the inner ring resonates at 956 MHz (catering to the RFID bands used in Europe and Japan respectively), hence providing dual-band response. The two rings are simultaneously excited by the arc-shaped feeding strip with the IC chip using microstrip-line coupling method [16]. The input impedance of conventional microstrip antennas is usually designed to match the 50 Ω impedance of the traditional feeder. However, in UHF RFID tags, the microchips have capacitive input impedance. Therefore, to enable maximum power transfer, the tag antenna must be designed to have inductive impedance for conjugate matching. The proposed antenna uses the commercially available Impinj Monza 4 tag chip (threshold power $P_{th} = -17.4$ dBm), which has impedances of $13 - j151\Omega$ at 866 MHz and $10 - j137\Omega$ at 956 MHz [17].

2. ANTENNA DESIGN

The geometry of the proposed RFID tag antenna is shown in Figure 1. It has two eccentric circular ring patches. An arc-shaped strip in between these two rings serves as the feeding strip and excites both the rings simultaneously. An eccentric circular ring patch covers smaller copper area than a regular circular patch. Therefore, it stores less energy beneath it than a circular patch of the same radius owing to its smaller dimension. This reduces the quality factor as the quality factor is directly related to the stored energy and is given by the equation:

$$Q = 2\pi \times \frac{\text{energy stored}}{\text{energy dissipated per cycle}} \tag{1}$$

With a decrease in the quality factor, the bandwidth increases as the quality factor is inversely proportional to the bandwidth [18]. Thus, the eccentric circular rings lead to bandwidth enhancement of the tag antenna. The entire design is printed on a commercially available 1.6 mm thick, inexpensive, FR-4 substrate of dielectric constant $\varepsilon_r = 4.4$ and loss tangent $\tan\delta = 0.002$. The overall size of the antenna is $91 \times 91\,\text{mm}^2$. The antenna design is simulated using Ansoft High Frequency Structure Simulator (HFSS) software. The optimized values of all the parameters are enlisted in Table 1.

The microchips used in UHF RFID tags have capacitive input impedance. For maximum power transfer, tag antennas are designed to have inductive impedance for conjugate matching. In order to achieve dual-band response, the impedances of the tag antenna must be matched with the chip impedances at both the resonant frequencies. The arc-shaped short-circuited microstrip-line structure consisting of the microchip (at an angle $\beta = 22^\circ$ with the x-axis) is used to excite the two rings simultaneously by coupling feed technique. It has been reported in the literature [16] that in coupling feed technique, the impedance of a tag antenna is contributed by the total length, width of the microstrip-line feeding structure and also the coupling distance between microstrip line and patch.

Table 1. Optimized values of the proposed tag antenna parameters.

Parameter	Values (mm)	Parameter	Values (mm)
L	91	r_1	59.9
W	91	r_2	46
R_1	39.4	r_3	26.6
R_2	35.4	r_4	23.4
R_3	31.9	t	2
R_4	24	d	0.75

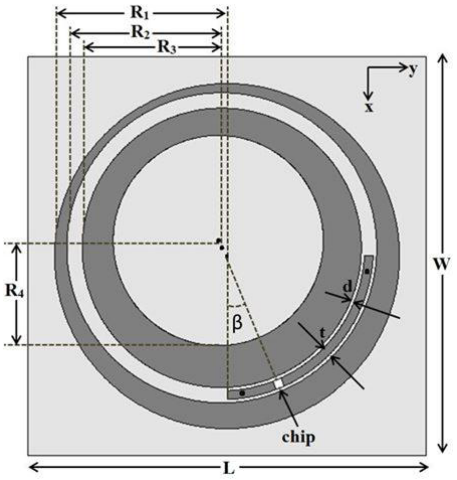

Figure 1. Design of the proposed antenna.

The reactive part of the tag antenna impedance is mainly determined by the inductive reactance of the short-circuited microstrip line. To acquire an inductive reactance of X_c, the required length (l) of the arc-shaped short-circuited microstrip line can be calculated using the formula [19]:

$$l = \frac{\lambda}{2\pi} \tan^{-1}\left(\frac{X_c}{Z_o}\right) \tag{2}$$

where λ is the free space wavelength at the operating frequency, and Z_o is the characteristic impedance of the short-circuited microstrip line. The value of Z_o of a microstrip line is approximated as follows [19]:

$$Z_o = \frac{60}{\sqrt{\varepsilon_e}} \ln\left(\frac{8h}{t} + \frac{t}{4h}\right) \quad \text{for} \quad \frac{t}{h} \leq 1 \tag{3}$$

where t is the width, and ε_e is the effective dielectric constant of the microstrip line.

Using Eq. (3) the characteristic impedance Z_o is calculated to be 63.6 Ω for the arc-shaped strip of thickness $t = 2$ mm. As the arc-shaped microstrip-line excites both the rings simultaneously, it is designed to obtain an impedance matching at an intermediate frequency of 911 MHz. By extrapolation, the chip impedance at 911 MHz is obtained to be around $11.16 - j143.65\Omega$. To obtain the reactance of $j143.65\Omega$, we have chosen the total length of the arc-shaped microstrip line to be 54.5 mm which is quite close to the value obtained from Eq. (2). The resistive part of the input impedance is 11.16 Ω and can be obtained by tuning the coupling distance d between the arc-shaped strip and the eccentric circular rings. Here, the coupling distance is chosen to be $d = 0.75$ mm. Two shorting pins, of radius 0.5 mm each, connect the arc-shaped feeding strip to the ground plane (of area 91×91 mm^2) on the opposite side of the substrate.

Initially, only the larger ring (Antenna 1) of outer radius, $r_1 = 59.9$ mm, and inner radius, $r_2 = 46$ mm, is taken and excited by the arc-shaped strip, as shown in Figure 2(a). It is found to

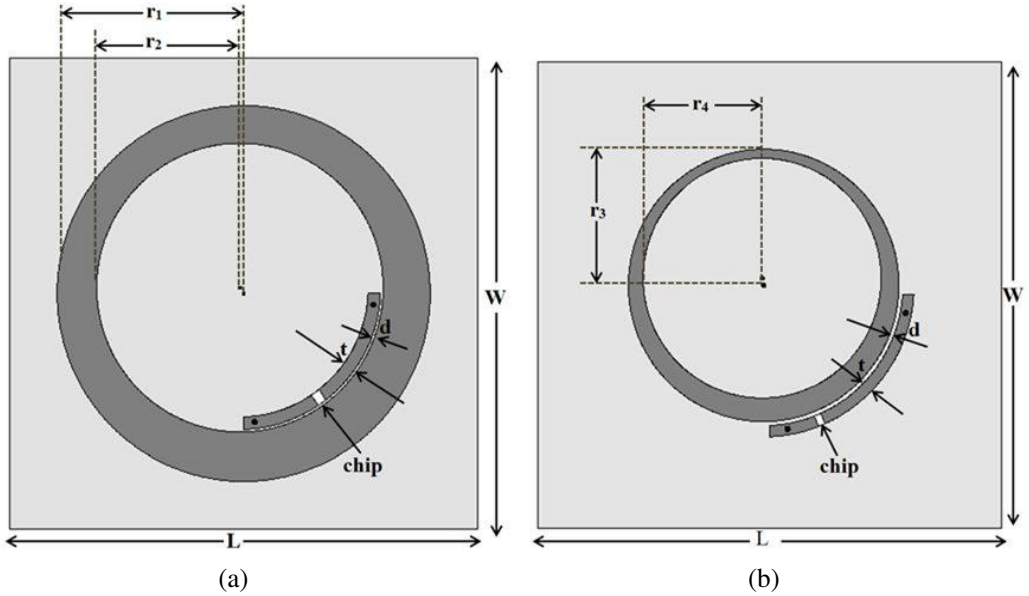

Figure 2. (a) Antenna 1 with only the larger ring (for 866 MHz). (b) Antenna 2 with only the smaller ring (for 956 MHz).

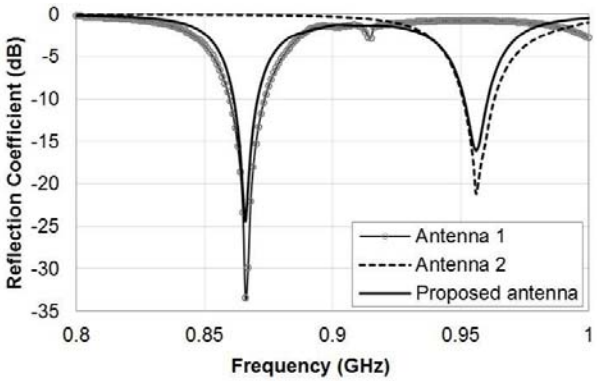

Figure 3. Reflection coefficients of Antenna 1, Antenna 2 and the proposed antenna.

resonate at 866 MHz with a reflection coefficient of −33.43 dB. Next, only the smaller ring (Antenna 2) of outer and inner radii, $r_3 = 26.6$ mm and $r_4 = 23.4$ mm, respectively, is considered with the feed structure, as shown in Figure 2(b). The inner ring resonates at 956 MHz. The value of the reflection coefficient at 956 MHz is −21.13 dB. Finally, by placing the smaller ring (outer radius, $R_3 = 31.9$ mm and inner radius, $R_4 = 24$ mm) inside the larger one (outer radius, $R_1 = 39.4$ mm, and inner radius, $R_2 = 35.4$ mm), dual-band operation is obtained at 866 MHz and 956 MHz, with each of the rings working as a single band resonator. The simulated return loss of the mono-band antennas and that of the proposed antenna are shown in Figure 3.

The surface current distributions of the proposed tag antenna at the higher and lower resonant frequencies are illustrated in Figure 4. From Figure 4, it can be clearly observed that at lower resonant frequency, i.e., at 866 MHz, the magnitude of current in the larger ring is more than that of the smaller ring, whereas the current distribution is more in the smaller ring than in the larger ring at the higher resonating frequency, i.e., at 956 MHz. Hence, it can be concluded that the smaller ring is responsible for resonance at the upper frequency band, and the larger ring is responsible for resonance at the lower frequency band.

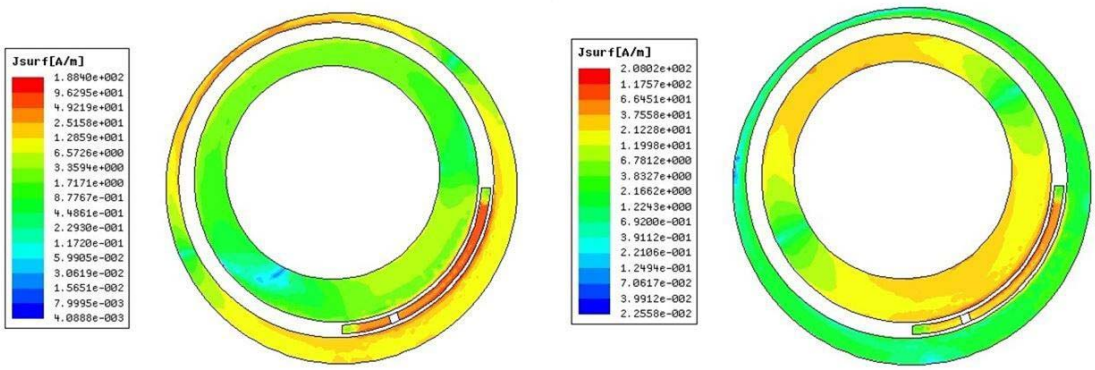

(a) (b)

Figure 4. Simulated surface current distribution on the eccentric circular rings at (a) 866 MHz and (b) 956 MHz.

3. PARAMETRIC ANALYSIS

3.1. The Effects of Varying R_1 and R_4

In the proposed dual-band tag antenna, the outer ring is responsible for the resonance at the lower band and the inner ring for the higher frequencyband. If R_1 is increased, keeping all other parameters constant, the dimension of the larger ring increases. This decreases the resonant frequency of the lower band. Figure 5 shows that with varying R_1 from 39.3 mm to 39.5 mm, the resonant frequency shifts from 869 MHz to 864 MHz without affecting the higher band. Similarly, by changing the value of R_4, keeping other parameters unchanged, the higher band can be tuned without much influence on the lower band. The effects of varying R_4 are shown in Figure 6. As R_4 is increased from 23.9 mm to 24.1 mm, the dimension of the smaller ring decreases, which in turn shifts the upper band resonating frequency from 952 MHz to 959 MHz.

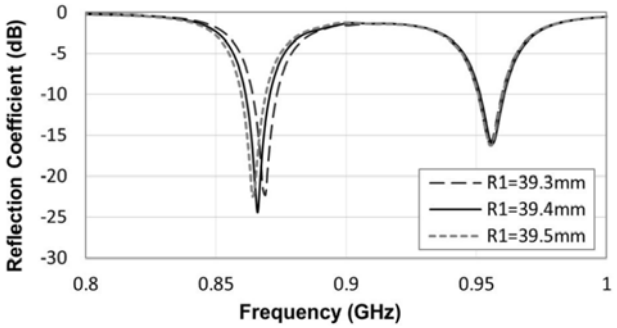

Figure 5. Effects of varying R_1 from 39.3 mm to 39.5 mm on the reflection coefficient.

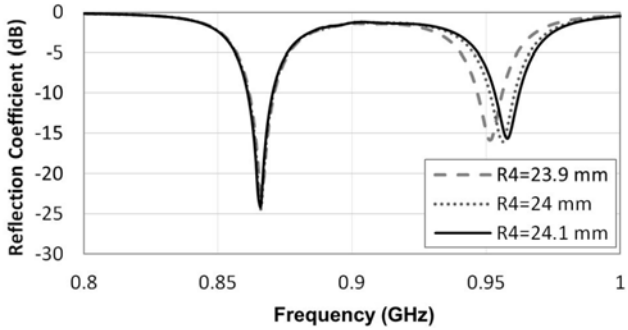

Figure 6. Effects of varying R_4 form 23.9 mm to 24.1 mm on the reflection coefficient.

3.2. The Effects of Tuning β

The chip is attached to the short-circuited microstrip feed-line making an angle β with positive x-axis. As β is decreased, both the real and imaginary parts of impedance increase. Thus, it is observed that with varying β proper impedance matching is obtained. Figure 7 shows different positions of the chip as β is decreased from 45° to 22°, and their corresponding impedances are plotted in Figure 8. The best impedance matching is obtained at $\beta = 22°$ where the simulated impedances of the antenna are found

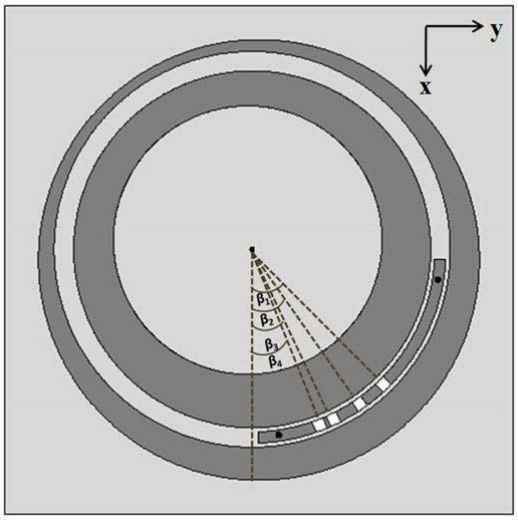

Figure 7. The proposed antenna showing different positions of the chip as β is varied from 45° to 22°.

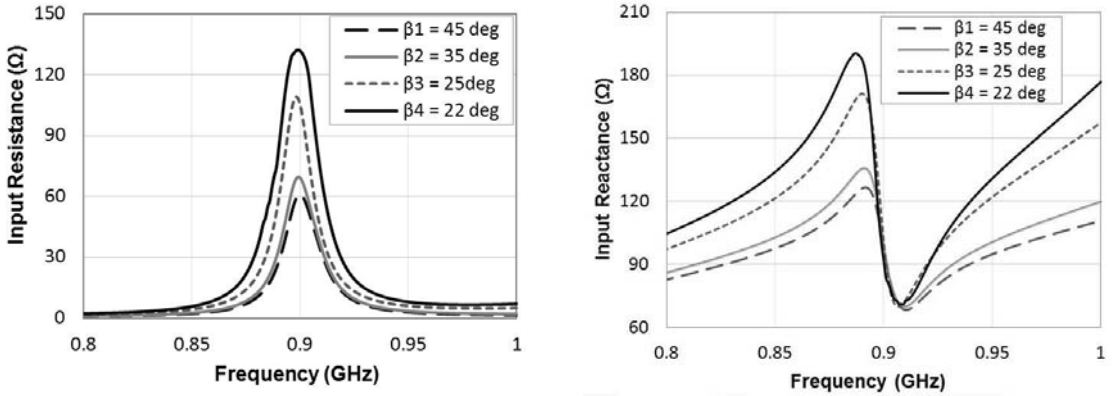

(a) (b)

Figure 8. Variation in the (a) input resistance (b) input reactance of the proposed antenna on decreasing β from 45° to 22°.

to be $11.7 + j151.7\Omega$ at 866 MHz and $7.3 + j136.7\Omega$ at 956 MHz resulting in return losses of -24.4 dB and -16.1 dB, respectively.

4. RESULTS AND DISCUSSION

4.1. Reflection Coefficient

The proposed dual-band tag antenna is fabricated by using the standard etching technique with PCB Prototyping machine (LPKF ProtoMat S103). Figure 9 shows the fabricated antenna. Of the different input impedance measurement techniques that can be employed for RFID tag antennas (viz., using baluns probes, mirror theories, differential probe [20, 21]), the differential probe method is used here to measure the input impedance at both the frequencies. Anritsu vector network analyzer (Model No. MS2038C) is used for the measurement of the input impedance through differential probes as shown in Figure 10. Figure 11 shows the simulated and measured impedance plots of the antenna. The simulated impedances of the antenna are found to be $11.7 + j151.7\Omega$ at 866 MHz and $7.3 + j136.7\Omega$ at 956 MHz, and the measured values are $21.2 + j149.2\Omega$ and $14 + j143.6\Omega$ at 866 MHz and 956 MHz,

respectively. Figure 12 depicts the simulated and measured reflection coefficients. The simulated values of the reflection coefficient are −24.4 dB at 866 MHz and −16.10 dB at 956 MHz, whereas the measured values of the same are −12.25 dB and −12.99 dB at 866 MHz and 952 MHz, respectively. The simulated and measured results are found in good agreement with each other. From Figure 12 it is observed that the measured 10 dB bandwidth is 9 MHz from 862 to 870 MHz and 8 MHz in the range of 949–956 MHz covering the UHF RFID bands used in Europe and Japan.

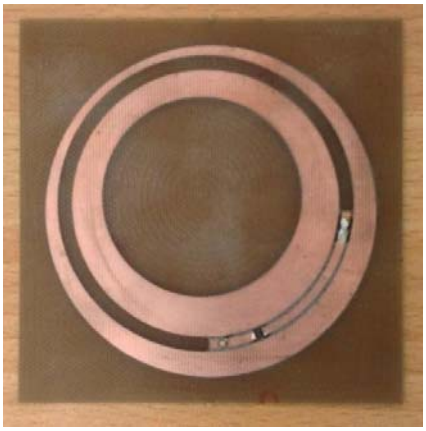

Figure 9. Fabricated antenna.

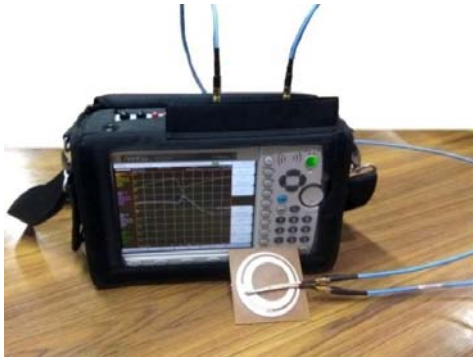

Figure 10. Measurement setup using VNA.

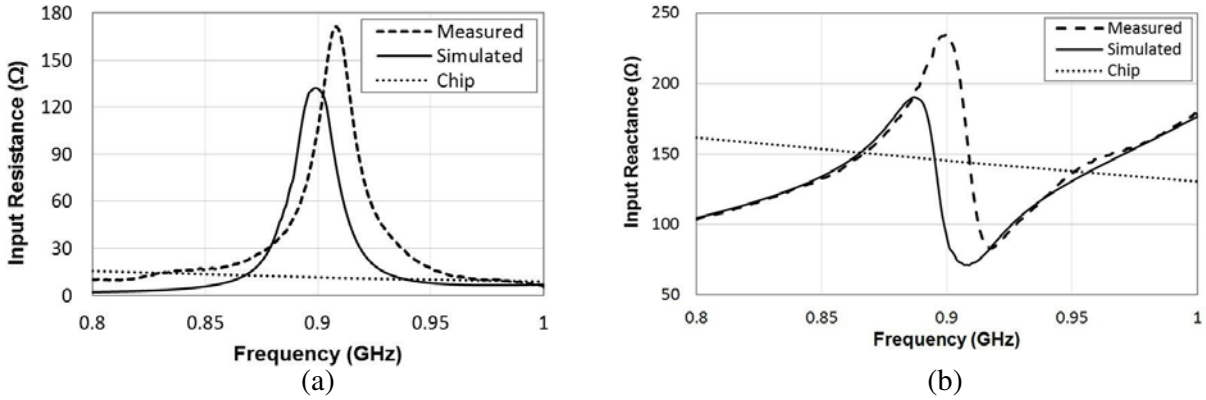

Figure 11. Measured and simulated (a) input resistance (b) input reactance of the proposed antenna.

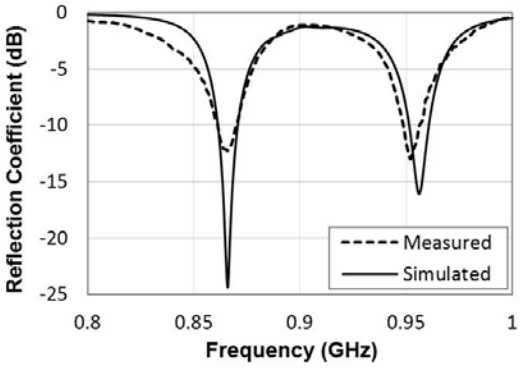

Figure 12. Simulated and measured reflection coefficients of the proposed antenna.

4.2. Read Range

To calculate the read range of the tag, Friis' free-space formula [22] is used, as given below:

$$r = \frac{\lambda}{4\pi}\sqrt{\frac{P_t G_t G_r \tau}{P_{th}}} \tag{4}$$

where λ is the wavelength; P_t is the power transmitted by the reader; G_t and G_r are the gains of the transmitting and receiving antennas, respectively; P_{th} is the minimum threshold power required to activate the RFID tag IC chip (for Impinj Monza 4 IC chip, $P_{th} = -17.4\,\text{dBm}$); τ is the power transmission coefficient which is given by,

$$\tau = \frac{4R_{chip}R_a}{|Z_a + Z_{chip}|^2}, \quad 0 \le \tau \le 1 \tag{5}$$

where $Z_{chip} = R_{chip} + jX_{chip}$ is the impedance of the IC chip, and $Z_a = R_a + jX_a$ is the impedance of the tag antenna. The product of the power transmitted by the reader and the gain of the transmitting antenna (i.e., P_tG_t) is the transmitter's effective isotropically radiated power (EIRP), which is allotted for different regions as per the International Telecommunication Union frequency regulations. The value of EIRP in European frequencies is 3.3 W, whereas in Japan it is 4 W [23]. The simulated gain of the antenna at different values of frequency is plotted in Figure 13. Using these values of gain, the read

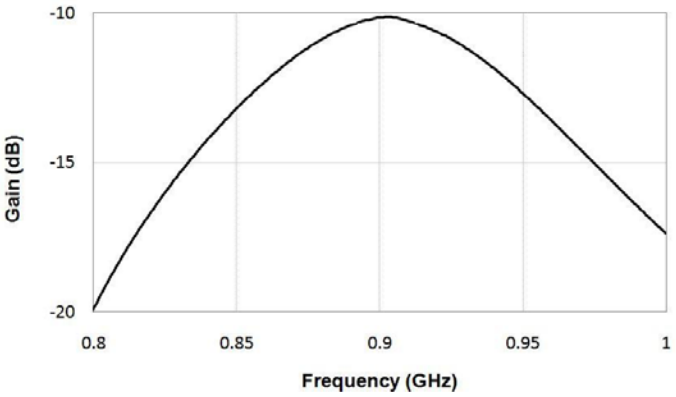

Figure 13. Simulated gain versus frequency plot of the proposed antenna.

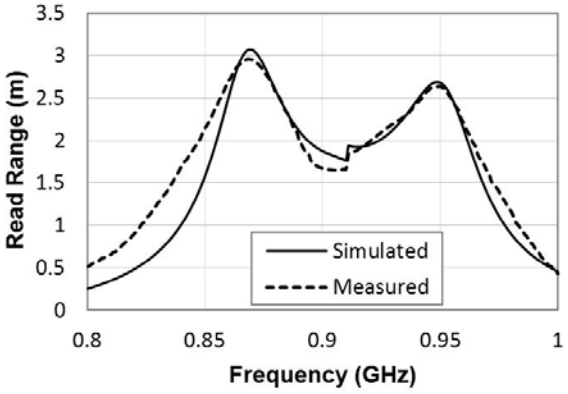

Figure 14. Simulated and measured read ranges.

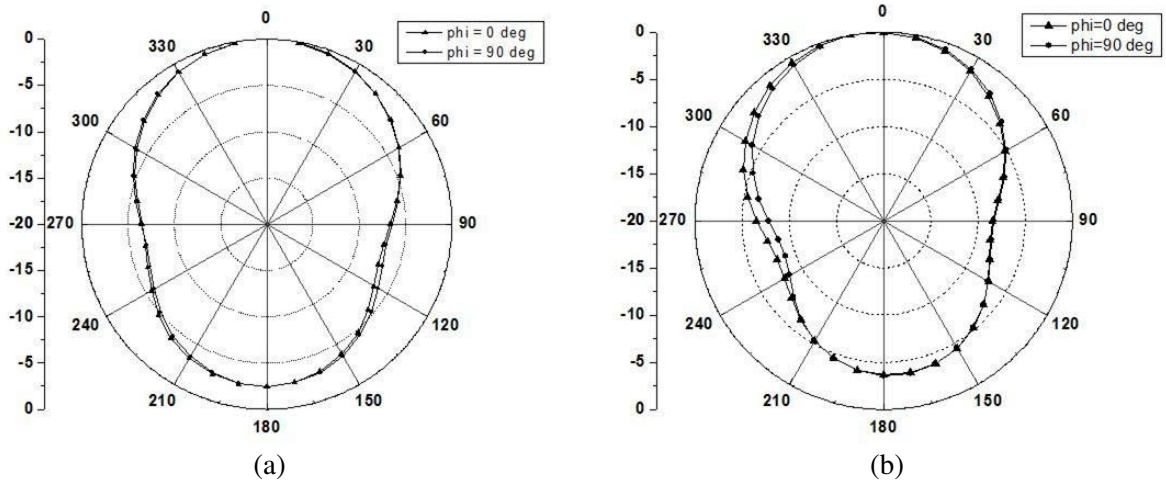

Figure 15. Radiation patterns at (a) 866 MHz (b) 956 MHz.

range is calculated at each frequency by employing Eq. (4). The plots of the measured and theoretical read ranges of the proposed antenna are shown in Figure 14. The theoretical and measured read ranges in the 865–868 MHz band and 950–956 MHz band are found around 3 m and 2.6 m, respectively.

4.3. Radiation Pattern

The radiation patterns of the antenna at 866 MHz and 956 MHz are simulated and found bidirectional, which are desirable for RFID applications. Figure 15 shows the simulated radiation patterns at both the frequencies.

A comparison of the proposed antenna with some of the UHF dual-band RFID tag antennas reported in the literature is shown in Table 2. Although the antennas reported in [24, 25] are smaller in dimension than the proposed antenna, considerable increment in the read range has been achieved in the designed antenna.

Table 2. Comparison of the proposed antenna with the previously reported UHF dual-band RFID tag antennas.

Published Literature	Antenna Size (mm^2)	Operating Bands	Read Range (m)
[24]	20×33.5	865–868 MHz	0.75
		908.5–914 MHz	1.6
[25]	65×52	860 MHz	2.5
		920 MHz	2
Proposed Antenna	91×91	865–868 MHz	3
		950–956 MHz	2.6

5. CONCLUSION

A UHF dual-band RFID tag antenna, operating at 866 MHz and 956 MHz bands allocated for the use in Europe and Japan, respectively, is designed and fabricated. The antenna consists of two eccentric circular rings where each of the rings resonates at one of these operating bands. Both the rings are excited simultaneously by a short-circuited arc-shaped strip (to which the RFID tag chip is attached) by microstrip-line coupling-feed technique. The simulated and measured reflection coefficients of the antenna are in good agreement with each other. The measured read ranges of the antenna are found around 3 m in 865–868 MHz band and 2.6 m in 950–956 MHz band. Bidirectional radiation patterns are obtained at both the frequencies rendering it useful for different RFID applications in both Europe and Japan.

ACKNOWLEDGMENT

The authors Bidisha Barman and Sudhir Bhaskar would like to thank Ministry of Human Resource Development (MHRD), Government of India, for funding the research through Teaching Assistantship (TA) programme.

REFERENCES

1. Tsai, M. C., C. W. Chiu, H. C. Wang, and T. F. Wu, "Inductively coupled loop antenna design for UHF RFID on-body applications," *Progress In Electromagnetics Research*, Vol. 143, 315–330, 2013.
2. Bhaskar, S., S. Singhal, and A. K. Singh, "Folded-slot active tag antenna for 5.8 GHz RFID applications," *Progress In Electromagnetics Research C*, Vol. 82, 89–97, 2018.
3. Nekoogar, F. and F. Dowla, *Ultra-Wideband Radio Frequency Identification Systems*, Springer, 2011.

4. Heidrich, J., D. Brenk, J. Essel, S. Schwarzer, K. Seemann, G. Fischer, and R. Weigel, "The roots, rules, and rise of RFID," *IEEE Microwave Magazine*, Vol. 2, No. 3, 78–86, May 2010.
5. Rao, K. V. S., P. V. Nikitin, and S. F. Lam, "Antenna design for UHF RFID tags: a review and a practical application," *IEEE Transactionon Antenna and Propagation*, Vol. 53, No. 12, 3870–3876, December 2005.
6. Hunt, V. D., A. Puglia, and M. Puglia, *RFID: A Guide to Radio Frequency Identification*, John Wiley & Sons, Inc., New York, 2007.
7. Paredes, F., G. Z. Gonzàlez, J. Bonache, and F. Martín, "Dual-band impedance-matching networks based on split-ring resonators for applications in RF Identification (RFID)," *IEEE Transactions on Microwave Theory And Techniques*, Vol. 58, No. 5, 1159–1166, May 2010.
8. Chen, J. S. and K. L. Wong, "A single-layer dual-frequency rectangular microstrip patch antenna using a single probe feed," *Microwave and Optical Technology Letters*, Vol. 11, No. 2, 38–84, 1996.
9. Liang, Z. X., D. C. Yang, X. C. Wei, and E. P. Li, "Dual-band dual circularly polarized microstrip antenna with two eccentric rings and an arc-shaped conducting strip," *IEEE Antennas Wireless Propagation Letters*, Vol. 15, 834–837, 2016.
10. Croq, F. and D. Pozar, "Multifrequency operation of microstrip antennas using aperture coupled parallel resonators," *IEEE Transactions on Antennas and Propagation*, Vol. 40, No. 11, 1367–1374, November 1992.
11. Richards, W. F., S. E. Davidson, and S. A. Long, "Dual-band reactively loaded microstrip antenna," *IEEE Transactions on Antennas and Propagation*, Vol. 33, No. 5, 556–560, May 1985.
12. Nakano, H. and K. Vichien "Dual-frequency square patch antenna with rectangular notch," *Electronics Letters*, Vol. 25, No. 16, 1067–1068, August 1989.
13. Yazidi, M. L., M. Himdi, and J. P. Daniel, "Aperture coupled microstrip antenna for dual frequency operation," *Electronics Letters*, Vol. 29, No. 17, 1506–1508, August 1993.
14. Paredes, F., G. Zamora, S. Zuffanelli, F. J. Herraiz-Martinez, F. Martin, and J. Bonache, "Free-space and on-metal dual-band tag for UHF-RFID applications in Europe and US," *Progress In Electromagnetics Research*, Vol. 141, 577–590, 2013.
15. Kim, D. and J. Yeo, "Dual-band long-range passive RFID tag antenna using an AMC ground plane," *IEEE Transactions on Antennas and Propagation*, Vol. 60, No. 6, 2620–2626, June 2012.
16. Kuo, S. H., H. D. Chen, S. C. Pan, Y. M. Tseng, and J. L. Jheng, "Compact circularly polarized circular microstrip tag antennamountable on metallic surface," *Microwave and Optical Technology Letters*, Vol. 55, No. 5, 1107–1112, May 2013.
17. Impinj Monza Tag Chip, Available Online: http://www.impinj.com.
18. Kumar, G. and K. P. Ray, *Broadband Microstrip Antennas*, Artech House, 2003.
19. Pozar, D. M., *Microwave Engineering*, 3rd Edition, Wiley, New York, 2005.
20. Kuo, S. K., S. L. Chen, and C. T. Lin, "An accurate method for impedance measurement of RFID tag antenna," *Progress In Electromagnetics Research*, Vol. 83, 9–106, 2008.
21. Zhu, H., Y. C. A. Ko, and T. T. Ye, "Impedance measurement for balanced UHF RFID tag antennas," *IEEE Radio and Wireless Symposium*, 128–131, 2010.
22. Marrocco, G., "The art of UHF RFID antenna design: Impedance matchingand size-reduction techniques," *IEEE Antennas and Propagation Magazine*, Vol. 50, No. 1, 66–79, February 2008.
23. Chawla, V. and D. S. Ha, "An overview of passive RFID," *IEEE Communications Magazine*, Vol. 45, No. 9, 11–17, September 2007.
24. Park, J. Y. and J. M. Woo, "Miniaturized dual-band S-shaped RFID tag antenna mountable on metallic surface," *Electronics Letters*, Vol. 44, No. 23, 1339–1341, November 2008.
25. He, Y. and B. Zhao, "A novel UHF RFID dual-band tag antenna with inductively coupled feed structure," *IEEE Wireless Communications and Networking Conference (WCNC)*, 2739–2743, Shanghai, China, 2013.